Trans-influences in mononuclear cyclopalladated compounds containing a $\sigma(Pd-C_{sp^2}$, ferrocene) bond. X-ray crystal structures of $[Pd\{[(\eta^5-C_5H_3)-CH=N-CH_2-C_6H_5]Fe(\eta^5-C_5H_5)\}(X)(PPh_3)]$ with $X^- = Br^-$ and I^-

Sonia Pérez [a], Ramon Bosque [a], Concepción López [a,*], Xavier Solans [b], Mercé Font-Bardia [b]

[a] *Departament de Quimica Inorgánica, Facultat de Quimica, Universitat de Barcelona, Martí i Franquès 1-11, E-08028 Barcelona, Spain*
[b] *Departament de Cristal lografia, Mineralogia i Dipòsits Minerals, Facultat de Geologia, Universitat de Barcelona, Martí i Franquès s/n, E-08028 Barcelona, Spain*

Abstract

The syntheses, characterization and study of the properties of cyclopalladated compounds of general formula: $[Pd\{(\eta^5-C_5H_3)-CH=N-CH_2-C_6H_5]Fe(\eta^5-C_5H_5)\}(X)(PPh_3)]$ with $X^- = Cl^-$, Br^-, I^-, CN^-, SCN^- or AcO^- are reported. Compounds with $X^- = Br^-$ and I^- were characterized by X-ray diffraction, and their crystal structures revealed the existence of a weak $C-H\cdots X$ interaction involving one of the $-CH_2-$ type hydrogen atoms bound to the imine nitrogen. Comparison of the spectroscopic properties of these compounds has allowed us to elucidate the influence of the monoanionic ligand, X^-, on a *trans*-arrangement to the metallated carbon atom upon the environment of the iron(II). Theoretical studies based on the semiempirical PM3(tm) were also been carried out to clarify the effects produced by the X^- ligand on the ring current of the metallated C_5H_3 ring of the ferrocenyl fragment. © 2001 Elsevier Science B.V. All rights reserved.

1. Introduction

Previous studies on cyclopalladated complexes containing *N*-donor ferrocenyl moieties of general formula: $[Pd\{[(\eta^5-C_5H_3)-C(R)=N-R']Fe(\eta^5-C_5H_5)\}Cl(L)]$ (with R = H, Me or Ph and R′ = phenyl or benzyl groups, and L = phosphine ligand) (Fig. 1) [1,2] have shown the effect of the electronic properties of the neutral L group upon the proclivity of the ferrrocenyl fragment to undergo oxidation [3–6]. In particular, the replacement of the PPh$_3$ in: $[Pd\{[(\eta^5-C_5H_3)-CH=N-CH_2-C_6H_5]Fe(\eta^5-C_5H_5)\}Cl(PPh_3)]$ by a more basic phosphine ligand such as PEt$_3$ [7] causes a decrease of the energy of the d–d

transition in the visible-ultraviolet spectrum and a decrease of the half-wave potential $[E_{1/2}(Fc)]$ of the ferrocenyl fragment, i.e. the iron becomes more prone to oxidation [6].

Fig. 1. Schematic view of compounds under study.
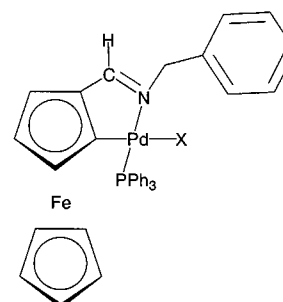
* Corresponding author. Tel.: +34-93-4021274; fax: +34-93-4907725.

E-mail address: conchi.lopez@qi.ub.es (C. López).

Table 1
Electronic and steric parameters of the monoanionic ligands, X [a]

X	σ_I	σ_R	ES–CH
Cl	0.51	−0.23	0.55
Br	0.50	−0.23	0.65
I	0.44	−0.22	0.78
CN	0.61	0.09	0.40
SCN	0.55	−0.05	
AcO	0.44	−0.24	0.50

[a] σ_I and σ_R are inductive (*para*) and mesomeric (*para*) values for the X groups and the ES–CH values are Charton's steric parameters calculated according to structural data. All the parameters presented in this table were obtained from Ref. [8].

However, the influence of the nature of the monoanionic ligand (X⁻), in a *trans*-arrangement to the metallated carbon atom of the ferrocenyl fragment, on the spectroscopic and structural properties of this sort of compound, has not yet been clarified. On this basis we decided to compare the properties of $[Pd\{[(\eta^5-C_5H_3)-CH=N-CH_2-C_6H_5]Fe(\eta^5-C_5H_5)\}(Cl)(PPh_3)]$ reported previously [1], with properties of the new derivatives: $[Pd\{[(\eta^5-C_5H_3)-CH=N-CH_2-C_6H_5]Fe(\eta^5-C_5H_5)\}(X)(PPh_3)]$, containing X⁻ = Br⁻, I⁻, CN⁻, SCN⁻ or AcO⁻, which differ exclusively in the electronic and steric properties (Table 1) [8] of the monoanionic ligand X⁻ bound to the palladium.

2. Results and discussion

2.1. Syntheses of the compounds

The new monomeric complexes $[Pd\{[(\eta^5-C_5H_3)-CH=N-CH_2-C_6H_5]Fe(\eta^5-C_5H_5)\}(X)(PPh_3)]$, with X⁻ = Br⁻, I⁻, CN⁻ and SCN⁻ were obtained by a ligand exchange procedure which consisted in the reaction of $[Pd\{[(\eta^5-C_5H_3)-CH=N-CH_2-C_6H_5]Fe(\eta^5-C_5H_5)\}(Cl)(PPh_3)]$ [1,2] with the stoichiometric amount of AgNO₃ in acetone to produce the precipitation of AgCl, followed by the addition of the stoichiometric amount of the corresponding potassium salt, KX {with X⁻ = Br⁻, I⁻, CN⁻ or SCN⁻} to the filtrate, and the subsequent purification of the compound by SiO₂-column chromatography (Scheme 1).

This procedure allowed us to isolate compounds $[Pd\{[(\eta^5-C_5H_3)-CH=N-CH_2-C_6H_5]Fe(\eta^5-C_5H_5)\}(X)(PPh_3)]$, with X⁻ = Br⁻, CN⁻ and SCN⁻ in fairly reasonable yields, but $[Pd\{[(\eta^5-C_5H_3)-CH=N-CH_2-C_6H_5]Fe(\eta^5-C_5H_5)\}(I)(PPh_3)]$ was obtained in low yield (ca. 15%). Attempts to prepare $[Pd\{[(\eta^5-C_5H_3)-CH=N-CH_2-C_6H_5]Fe(\eta^5-C_5H_5)\}(AcO)(PPh_3)]$ using this procedure failed.

To improve the yield of the preparation of $[Pd\{[(\eta^5-C_5H_3)-CH=N-CH_2-C_6H_5]Fe(\eta^5-C_5H_5)\}(I)(PPh_3)]$, an alternative strategy was adopted. This consisted in the conversion of $[Pd\{[(\eta^5-C_5H_3)-CH=N-CH_2-C_6H_5]Fe(\eta^5-C_5H_5)\}(\mu-Cl)]_2$ into the corresponding di-μ-iodo-bridged dinuclear complex: $[Pd\{[(\eta^5-C_5H_3)-CH=N-CH_2-C_6H_5]Fe(\eta^5-C_5H_5)\}(\mu-I)]_2$, and its subsequent treatment with PPh₃ in a 1:2 molar ratio (Scheme 2).

$[Pd\{[(\eta^5-C_5H_3)-CH=N-CH_2-C_6H_5]Fe(\eta^5-C_5H_5)\}(AcO)(PPh_3)]$ was synthesised successfully with a two-step sequence of reactions (Scheme 3). The first step was reaction of the ferrocenylimine $[(\eta^5-C_5H_5)Fe\{(\eta^5-C_5H_3)-CH=N-CH_2-C_6H_5\}]$ [1] with the equimolar amounts of Pd(AcO)₂ and NaAcO·3H₂O, which yielded $[Pd\{[(\eta^5-C_5H_3)-CH=N-CH_2-C_6H_5]Fe(\eta^5-C_5H_5)\}(\mu-AcO)]_2$. This reaction involved the activation of the $\sigma(C_{sp^2}, ferrocene-H)$ bond. In the second step, the addition of PPh₃ to a suspension of dimeric complex in acetone, produced the cleavage of the 'Pd(μ-AcO)₂Pd' units to give: $[Pd\{[(\eta^5-C_5H_3)-CH=N-CH_2-C_6H_5]Fe(\eta^5-C_5H_5)\}(AcO)(PPh_3)]$.

2.2. Characterization

All the compounds prepared in this study were orange or red solids at room temperature. The monomeric compounds are highly soluble in CH₂Cl₂, CHCl₃, benzene and acetone, but they have lower solubility in alcohols and alkanes. The di-μ-iodo- and the di-μ-acetato-bridged cyclopalladated complexes have low solubility in the most common solvents. All the compounds were characterized by elemental analy-
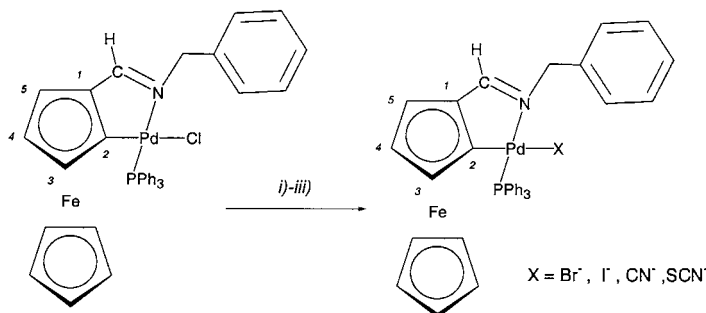
Scheme 1.
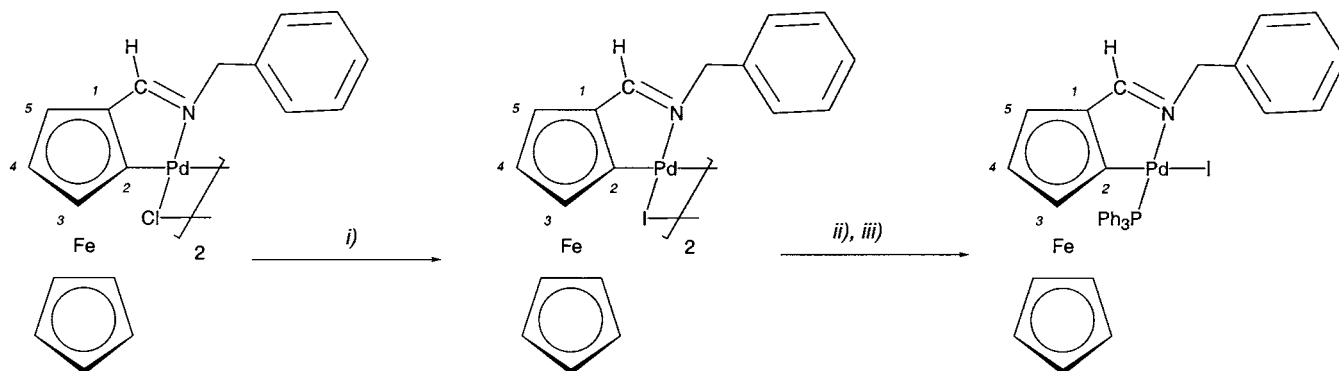
Scheme 2.
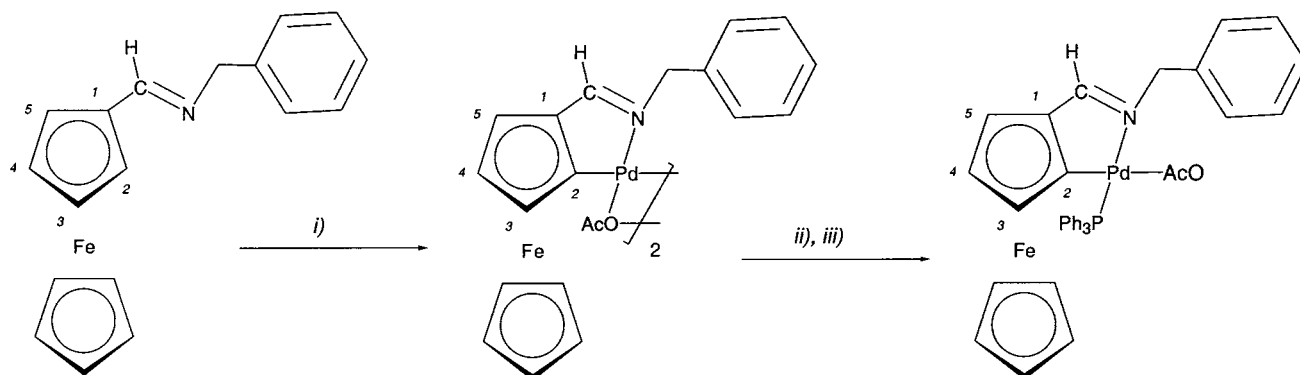
Scheme 3.

ses and in all cases the experimental data confirmed the proposed formula (see Section 3). The most outstanding features observed in the infrared spectra of these compounds is the presence of a sharp and intense band in the range 1570–1595 cm^{-1}, which is assigned to the asymmetric stretching of the $>C=N-$ group. This absorption appears at lower wavenumbers than in the free ferrocenylaldimine [$v(>C=N-) = 1625$ cm^{-1}] [1,2] due to the coordination of the ligand. In all cases, the typical bands of the coordinated triphenylphosphine [9] were also observed and the IR spectra of compounds [Pd{[(η^5-C_5H_3)–CH=N–CH_2–C_6H_5]Fe(η^5-C_5H_5)}(X)-(PPh$_3$)] with X$^-$ = CN$^-$ or SCN$^-$ also showed the bands due to these functional groups (at ca. 2091 and 2145 cm^{-1}, respectively). The IR spectra of: [Pd{[(η^5-C_5H_3)–CH=N–CH_2–C_6H_5]Fe(η^5-C_5H_5)}(AcO)(PPh$_3$)] showed $v_{asym.}$ (CO$_2$) and $v_{sym.}$ (CO$_2$) separated by 278 cm^{-1}, which is consistent with unidentate acetate coordination [10]. The mononuclear compounds were characterized by ^{1}H and and ^{13}C{^{1}H}-NMR spectroscopy (Tables 2 and 3). The signals were assigned with the aid of two-dimensional heteronuclear {^{1}H-^{13}C}-NMR experiments. In all cases, the number of signals observed in the ^{1}H-NMR spectra and their multiplicities (Table 2) were consistent with the patterns expected for 1,2-disubstituted ferrocenyl ligands having a σ(Pd–C_{sp^2})

Table 2
Selected ^{1}H-NMR data (in ppm) for compounds for [Pd{[(η^5-C_5H_3)–CH=N–CH_2–C_6H_5]Fe(η^5-C_5H_5)}(X)(PPh$_3$)] (labelling of the atoms refers to those shown in Schemes 1–3)

X	C_5H_5	H^3	H^4	H^5	–CH_2– [a]	–CH=N– [b]
Cl	3.67	3.31	4.02	4.29	4.63 5.41	7.90
Br	3.65	3.36	3.99	4.27	4.77 5.50	7.93
I [c]	3.67	3.42	3.99	4.27	5.03 5.67	7.07
CN	3.80	3.52	4.09	4.33	4.57 4.73	7.86
SCN [c]	3.72	3.29	4.06	4.31	4.64 5.00	7.93
AcO	3.69	3.45	4.02	4.25	4.51 4.82	[d]

[a] The two protons of this group are diastereotopic.
[b] Doublet due to phosphorus coupling, ^3J(P–H) in the range 7.5–8.0 Hz.
[c] Additional singlet at ca. 5.12 ppm due to the CH$_2$Cl$_2$ of crystallization.
[d] Overlapped by the multiplet due to the aromatic protons of the PPh$_3$ ligand.

Table 3
Selected $^{13}C\{^1H\}$-NMR data (in ppm) for compounds $[Pd\{[(\eta^5-C_5H_3)-CH=N-CH_2-C_6H_5]Fe(\eta^5-C_5H_5)\}(X)(PPh_3)]$ (labelling of the atoms refers those shown in Schemes 1–3)

| X | ^{13}C-NMR | | | | | | | | ^{31}P-NMR |
	C_5H_5	C^1	C^2	C^3	C^4	C^5	$-CH_2-$	$-CH=N-$	$\delta(^{31}P)$
Cl	69.80	87.57	104.18	77.38	69.35	66.48	59.10	172.38	37.54
Br	69.82	87.68	107.03	77.40	69.14	66.34	62.90	172.52	37.75
I	69.93	87.72	108.72	76.54	68.94	66.23	64.25	172.88	37.93
CN	70.20	86.91	96.90	77.20	77.34	66.77	58.70	171.82	34.93
SCN	69.83	87.01	97.20	77.30	77.14	66.93	61.32	172.05	35.78
AcO [a]	69.79	87.41	98.00	77.40	77.55	66.36	58.98	172.12	36.47

[a] An additional signal at 23.42 ppm due to the CH_3 group of the acetato ligand was observed in the ^{13}C-NMR spectrum of this compound.

bond [1–4]. The resonance of the $N-CH_2-$ protons appeared as a doublet of doublets due to diastereopicity. The chemical shifts and the separation of these signals were strongly affected by the nature of the ligand X.

Comparison of $^{13}C\{^1H\}$-NMR data revealed that the position of the signal due to the metallated carbon atom, C^2, is strongly sensitive (ca. 12 ppm) to the nature of the monoanionic group (X^-) on a *trans*-arrangement (Table 3). The chemical shifts of this signal increased according to the sequence:

$$CN^- < SCN^- < AcO^- < Cl^- < Br^- < I^- \qquad (1)$$

Similar trends were also found for the resonances of the imine carbon and of C^1, but in these cases the variations for all the compounds were smaller.

^{31}P-NMR spectra of compounds $[Pd\{[(\eta^5-C_5H_3)-CH=N-CH_2-C_6H_5]Fe(\eta^5-C_5H_5)\}(X)(PPh_3)]$ showed a singlet in the range 30–40 ppm (Table 3). This is consistent, according to the literature [1,2,6,11] with a *trans*-arrangement of the phosphine ligand and the nitrogen of the ferrocenyl Schiff base. As can be easily seen in Table 3, changes in the monoanionic group, X^-, in a *cis*-arrangement to the PPh_3 ligand, produced a shift of the signal to higher fields, which follows the trend:

$$CN^- < SCN^- < AcO^- < Cl^- < Br^- < I^- \qquad (2)$$

Although in this case the maximum variation is only of ca. 3 ppm, this sequence is formally identical to that found for the chemical shift of the metallated carbon atom (Eq. (1)). These equations provide a rough first approach to order the X^- ligands according to: (a) their *trans*- influence upon the metallated carbon, which is directly involved in the ring current of the ferrocenyl fragment, and (b) the effect produced by these groups on the electronic environment of the phosphorus atom of the PPh_3 ligand in a *cis*-orientation (*cis*-influences).

2.3. Description of the crystal structures of $[Pd\{[(\eta^5-C_5H_3)-CH=N-CH_2-C_6H_5]Fe(\eta^5-C_5H_5)\}(X)(PPh_3)]$ with $X^- = Br^-$ or I^-

Perspective drawings of the molecular structures of $[Pd\{[(\eta^5-C_5H_3)-CH=N-CH_2-C_6H_5]Fe(\eta^5-C_5H_5)\}(Br)(PPh_3)]$ and $[Pd\{[(\eta^5-C_5H_3)-CH=N-CH_2-C_6H_5]Fe(\eta^5-C_5H_5)\}(I)(PPh_3)]$, together with their atom labelling schemes are depicted in Figs. 2 and 3. A selection of bond lengths and angles is shown in Table 4.

These structures consist of discrete molecules of $[Pd\{[(\eta^5-C_5H_3)-CH=N-CH_2-C_6H_5]Fe(\eta^5-C_5H_5)\}(X)(PPh_3)]$ with $X^- = Br^-$ or I^-, separated by van der Waals contacts. In each molecule the palladium is in a slightly distorted square-planar environment coordinated with the bromo or iodo ligands, the phosphorus of the PPh_3 ligand, the nitrogen and the C10 atom (for $X^- = Br^-$) or the C6 atom (for $X^- = I^-$) of the ferrocenyl group. The PPh_3 ligand and the imine nitrogen are in a *trans*-arrangement in close accord with the results obtained by ^{31}P-NMR spectroscopy.

In compounds: $[Pd\{[(\eta^5-C_5H_3)-CH=N-CH_2-C_6H_5]Fe(\eta^5-C_5H_5)\}(X)(PPh_3)]$, the five-membered palladacycles, are practically planar, contain the imine group (endocyclic) and form angles of ca. 7.1° (for $X^- = Br^-$) and 5.4° (for $X^- = I^-$) with the C_5H_3 ring of the ferrocenyl.

In the two structures the imine adopts the anti-conformation and the $>C=N-$ bond lengths [1.281(5) Å (for $X^- = Br^-$) and 1.285(5) Å (for $X^- = I^-$)] does not differ significantly from the length reported for the free ligand [1.262(7) Å] [12].

The phenyl ring bound to the $-N-CH_2-$ portion is planar and the normal to its main plane forms angles of ca. 99.5° (for $X^- = Br^-$) or 101.96° (for $X^- = I^-$) with the imine moiety plane.

An interesting feature of the structures of $[Pd\{[(\eta^5-C_5H_3)-CH=N-CH_2-C_6H_5]Fe(\eta^5-C_5H_5)\}X(PPh_3)]$ is the short distance between the bromo or iodo ligands and the H12A atom of the $-N-CH_2-$ group [2.86 and 2.95 Å for $X^- = Br^-$ or I^-, respectively], which is

clearly less than the sum of the van der Waals radii of the two atoms involved {H, 1.20 Å and Br, 1.95 or I = 2.15 Å [13]}. This suggests a weak intramolecular C12–H12A···X {X = Br or I} interaction.

The two rings of the ferrocenyl unit are planar, nearly parallel [tilt angles of 4.2° (for $X^- = Br^-$) and 2.5° (for $X^- = I^-$)] and they deviate from the ideal eclipsed conformation by 9.2 and 4.6° for $X^- = Br^-$ and I^-, respectively. The distances between the palladium and the iron(II) are: 3.6028 Å (for $X^- = Br^-$) and 3.6750 Å (for $X^- = I^-$), which suggests that there is no direct interaction between them.

In a first attempt to elucidate whether the replacement of a Cl^- group in $[Pd\{[(\eta^5-C_5H_3)-CH=N-CH_2-C_6H_5]Fe(\eta^5-C_5H_5)\}(Cl)(PPh_3)]$ by bulkier and less electronegative (Table 1) X^- ligand ($X^- = Br^-$ or I^-) could cause significant modifications in the structures of this sort of compounds, a comparative study of selected bond lengths and angles of complexes $[Pd\{[(\eta^5-C_5H_3)-CH=N-CH_2-C_6H_5]Fe(\eta^5-C_5H_5)\}(X)(PPh_3)]$ with $X^- = Cl^-$ [14], Br^- and I^- was undertaken. Data shown in Table 4 revealed that, except for the Pd–X bond length and the Pd–N bond length, which increases according to the sequence $Cl^- < Br^- < I^-$, the remaining Pd-ligands' bond distances [Pd–P and Pd–C] are very similar (the differences do not clearly exceed 3σ). This also applies for the bond angles involving the metallated carbon bond. The major differences were found in the bond angles involving the X^- ligand. For instance, the P–Pd–X bond angle in the chloro derivative [95.4(1)°] is greater than in the bromo or iodo analogues [94.99(6)° (for $X^- = Br^-$) and 94.81(5)° (for $X^- = I^-$)]. This variation is compensated by a narrowing of the N–Pd–Cl bond angle [92.8(1)°] from the N–Pd–Br [93.75(9)°] or N–Pd–I [94.68(10)°] bond angles.

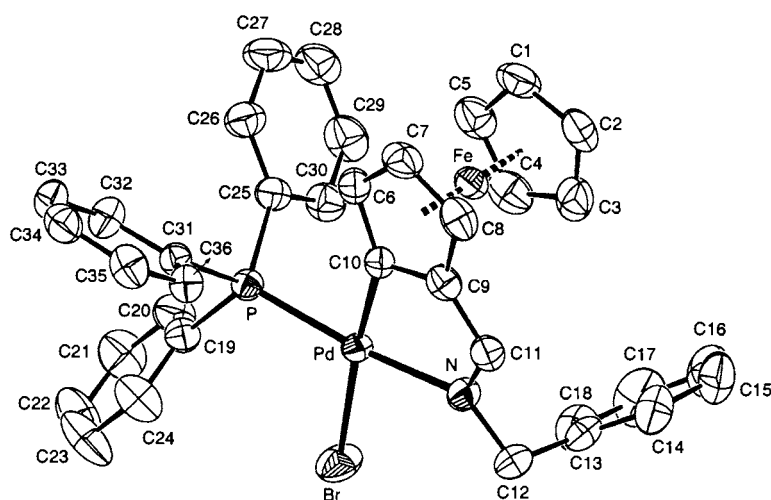Fig. 2. Molecular structure and atom labelling scheme for $[Pd\{[(\eta^5-C_5H_3)-CH=N-CH_2-C_6H_5]Fe(\eta^5-C_5H_5)\}(Br)(PPh_3)]$.
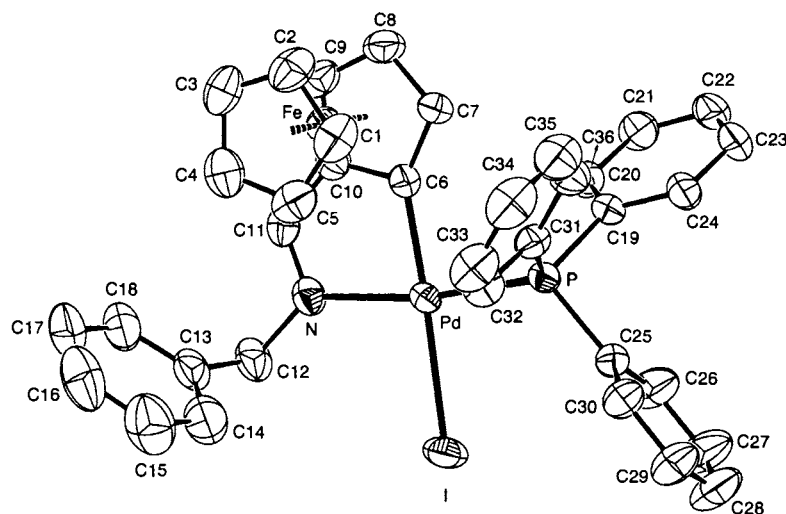
Fig. 3. Molecular structure and atom labelling scheme for for $[Pd\{[(\eta^5-C_5H_3)-CH=N-CH_2-C_6H_5]Fe(\eta^5-C_5H_5)\}(I)(PPh_3)]$.

Table 4

Selected bond lengths (Å) and bond angles (°) for compounds $[Pd\{[(\eta^5\text{-}C_5H_3)\text{-}CH=N\text{-}CH_2\text{-}C_6H_5]Fe(\eta^5\text{-}C_5H_5)\}(X)(PPh_3)]$ {with $X^- = Br^-$, I^- and Cl^- [a]} (standard deviations are given in parenthesis)

	$X^- = Br^-$	$X^- = I^-$	$X^- = Cl^-$
Bond lengths			
Pd–$C_{met.}$ [b]	2.012(3)	2.012(4)	2.004(5)
Pd–N	2.159(3)	2.172(3)	2.146(6)
Pd–P	2.2469(14)	2.2532(16)	2.247(2)
Pd–X	2.5040(17)	2.6640(13)	2.368(2)
N–C(11)	1.281(5)	1.285(5)	1.279(7)
Fe–C [c]	2.045(8)	2.047(9)	2.051(7)
C–C(ring) [c,b]	1.416(13)	1.421(13)	1.417(10)
Bond angles			
N–Pd–$C_{met.}$ [b]	80.50(13)	80.66(14)	80.8(2)
P–Pd–$C_{met.}$ [b]	90.74(11)	89.83(11)	91.0(2)
N–Pd(1)–X	93.75(9)	94.68(10)	92.8(1)
P(4)–Pd–X	94.99(6)	94.81(5)	95.4(1)

[a] Data from Ref. [19].

[b] $C_{met.}$ represents the metallated carbon atom: C(10) for $X^- = Br^-$ and C(6) for $X^- = I^-$.
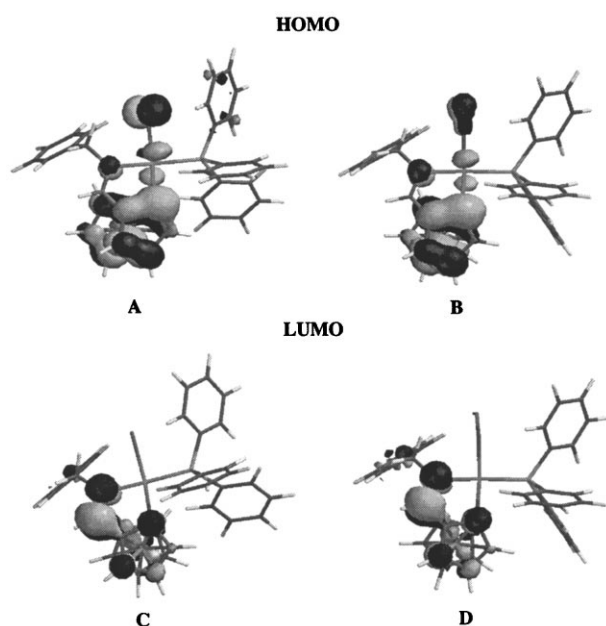
[c] Average values for the ferrocenyl moiety.

HOMO

LUMO

Fig. 4. HOMO of compounds $[Pd\{[(\eta^5\text{-}C_5H_3)\text{-}CH=N\text{-}CH_2\text{-}C_6H_5]Fe(\eta^5\text{-}C_5H_5)\}(X)(PPh_3)]$ {with $X = Br^-$ and CN^-} (A) and (B), respectively. The drawings labelled as (C) and (D) correspond to the LUMO of compounds with $X^- = Br^-$ or CN^-.

A careful study of the structural data reported for compound $[Pd\{[(\eta^5\text{-}C_5H_3)\text{-}CH=N\text{-}CH_2\text{-}C_6H_5]Fe(\eta^5\text{-}C_5H_5)\}(Cl)(PPh_3)]$ [19] suggests that, in this case too, the distance between the Cl^- and one of the protons of the $-N\text{-}CH_2-$ fragment is [2.83 Å] smaller than the sum of the van der Waals radii of these two atoms {Cl, 1.75 and H, 1.20 Å [13]}. This also suggests a weak

intramolecular C–H···Cl interaction. This may be related to the differences detected in the values of the bond angles: N–Pd–X and P–Pd–X described above. Since the effective bulks of the Br^- and I^- groups are [ES–CH = 0.65 (for Br^-) and 0.78 (for I^-) [8]] greater than the bulk of the Cl^- [ES–CH = 0.55 [8]] group, one would expect that the Br^- or the I^- groups would tend to move further away from the PPh_3 to reduce steric hindrance. However, in the bromo or iodo derivatives the P–Pd–X bond angles are [94.99(6)° (for $X^- = Br^-$) and 94.81(5)° (for $X^- = I^-$)] smaller than for the chloro analog [95.4(1)°]. The narrowing of the N–Pd–Cl bond angle causes, the Cl^- ligand to approach the H12A atom, which is involved in the intramolecular C–H···Cl interaction.

2.4. Theoretical approaches to clarify the influence of the ligand in a trans-arrangement to the metallated carbon upon the electronic environment of the Fe(II)

In a first attempt to understand the trends detected in the NMR spectra of the compounds holding different X^- groups upon the ferrocenyl unit, we decided to perform theoretical calculations to find out whether these monoanionic groups could cause significant variations in the electronic density of the ferrocenyl fragment. Previous studies have shown that for the ferrocenylamine $[(\eta^5\text{-}C_5H_5)Fe\{(\eta^5\text{-}C_5H_4)\text{-}CH_2\text{-}N(CH_3)_2\}]$, the Schiff bases $[(\eta^5\text{-}C_5H_5)\}Fe\{(\eta^5\text{-}C_5H_4)\text{-}C(CH_3)=N\text{-}R\}]$ {R = phenyl or benzyl groups} and their cyclopalladated complexes, the PM3(tm) model of the SPARTAN 5.0 program [15] provided optimized geometries which were in excellent agreement with the structural data obtained by X-ray diffraction [6]. On this basis, we assumed that this procedure could also be used for compounds $[Pd\{[(\eta^5\text{-}C_5H_3)\text{-}CH=N\text{-}CH_2\text{-}C_6H_5]Fe(\eta^5\text{-}C_5H_5)\}(Br)(PPh_3)]$.

For derivatives holding $X^- = Cl^-$, Br^- and I^-, whose structural data are available, the crystallographic coordinates were used as input for the optimization of the geometry, but no significant variations in either bond lengths, angles or other structural parameters were detected, thus indicating that the PM3(tm) model could also be extended to these systems.

As shown in Fig. 4A and B, the metallated carbon atom is directly involved in the HOMO, in addition to the contribution of the orbital(s) of the X^- ligand: a p orbital of the Cl^-, Br^-, I^-, or the sulfur of the SCN^- groups or the π-orbital of the CN^- ligand (Fig. 4A,B). These findings suggested that the electronic density of the metallated ring could be directly affected by the characteristics of the X^- ligand.

In a first approach to clarifying the effect of the X^- group on the ring current of the C_5H_3 ring, the average values of Mulliken's bond orders {here in after MBO} [16] for the C–C bonds of this ring were calculated for

all the compounds as well as for ferrocene and the free imine. In these systems the geometry chosen was the same as the geometry of these groups in the cyclometallated compound. The highest value of MBO corresponded to ferrocene, the intermediate was for the free imine and the lowest for the cyclometallated complexes. This is consistent with the electron-pulling nature of the imine and of the '[PdX(PPh$_3$)]' moieties [14]. For the cyclopalladated derivatives, the averaged value of Mulliken's bond order [16] increased upon changing the anionic group according to the sequence: $CN^- < SCN^- < Cl^- < Br^- < I^-$. This trend, which is formally identical to that shown in Eq. (1), reflects the increase of the electronic density of the C$_5$H$_3$, which is consistent with the lowfield shift of the signal due to the metallated carbon atom, C^2, in the ^{13}C{^{1}H}-NMR spectra.

In all cases, the LUMO is mainly formed by the combination of two π^* orbitals, one of the ferrocenyl fragment and the other of the imine group (Fig. 4 C,D). These results are consistent with those reported for: [Pd{[(η^5 - C$_5$H$_3$)–C(CH$_3$)=N–C$_6$H$_5$]Fe(η^5 - C$_5$H$_5$)}(Cl)(PH$_3$)] [6].

2.5. Conclusions

The results presented here have allowed us to establish *trans*-influence of the monoanionic ligand X$^-$ {Cl$^-$, Br$^-$, I$^-$, CN$^-$, SCN$^-$ or AcO$^-$} on the spectroscopic properties of cyclopalladated derivatives of general formula: [Pd{[(η^5-C$_5$H$_3$)–CH=N–CH$_2$–C$_6$H$_5$]Fe(η^5-C$_5$H$_5$)}(X)(PPh$_3$)]. The variations observed in the NMR spectra have been rationalized with the aid of semiempirical calculations performed with the SPARTAN 5.0 suite of programs [15]. The results revealed that changes of the X$^-$ ligand in a *trans*-arrangement to the metallated carbon made the electronic density of the C$_5$H$_3$ ring of the ferrocenyl moiety increase according to the sequence: $CN^- < SCN^- < Cl^- < Br^- < I^-$. This is consistent with the shift of the signal due metallated carbon atom, C^2, of the ferrocenyl fragment.

The comparison of the structural data for compounds: [Pd{[(η^5-C$_5$H$_3$)–CH=N–CH$_2$–C$_6$H$_5$]Fe(η^5-C$_5$H$_5$)}(X)(PPh$_3$)] with X$^-$ = Cl$^-$, Br$^-$, I$^-$, shows that although the Br$^-$ and I$^-$ groups are bulkier than the Cl$^-$ ligand (Table 1) the replacement of the Cl$^-$ ligand by a Br$^-$ or a I$^-$, does not produce significant variations in the bond lengths and angles of the metallacycle. In the three cases, the short distances between the X$^-$ ligand and one of the hydrogens, H12A, of the –N–CH$_2$– unit suggest a weak C12–H12A···X {X$^-$ = Cl$^-$, Br$^-$ or I$^-$} intramolecular interaction. The use of the SPARTAN 5.0 computer program [15], also indicated that for these compounds, this sort of interaction is expected to be attractive, since small changes ($\pm 10°$) in the N–Pd–X bond angles or in the torsion angles

Pd–N–C12–H12A caused a significant increase of the formation enthalpy, $\Delta H_{form.}$, of these complexes. Thus, these C–H···X intramolecular interactions appear to contribute to the stabilisation of these molecules.

3. Experimental

3.1. Materials and synthesis

The ligand [(η^5-C$_5$H$_5$)Fe{(η^5-C$_5$H$_3$)–CH=N–CH$_2$–C$_6$H$_5$}], the di-μ-chloro-bridged cyclopalladated complex [Pd{[(η^5-C$_5$H$_3$)–CH=N–CH$_2$-C$_6$H$_5$]Fe(η^5–C$_5$-H$_5$)}(μ-Cl)]$_2$ and compound [Pd{[(η^5-C$_5$H$_3$)–CH=N–CH$_2$–C$_6$H$_5$]Fe(η^5-C$_5$H$_5$)}(Cl)(PPh$_3$)] were prepared as described previously [1].

Elemental analyses {C, H, N and S (for SCN–derivative)} were carried out at the Serveis Cientifico-Tècnics de la Universitat de Barcelona. Infrared spectra were obtained with a Nicolet Impact 400 instrument using KBr disks. Proton and two-dimensional {^{1}H-^{13}C} heteronuclear NMR experiments were run at 500 MHz with either a Varian 500 or a Bruker advance 500DMX instrument. The solvent used for the NMR experiments was CDCl$_3$ (99.9%) and SiMe$_4$ was the internal reference. ^{31}P{^{1}H}-NMR spectra were recorded with a Bruker 250DXR instrument using CDCl$_3$ (99.9%) as solvent and P(OMe)$_3$ as internal reference [δ {P(OMe)$_3$ = 140.17 ppm]. In all cases, the chemical shifts (δ) are given in ppm and the coupling constants (J) in Hz.

3.1.1. Preparation of [Pd{[(η^5-C$_5$H$_3$)–CH=N–CH$_2$–C$_6$H$_5$]Fe(η^5-C$_5$H$_5$)}(μ-I)]$_2$

The di-μ-chloro-bridged cyclopalladated complex [Pd{[(η^5 - C$_5$H$_3$)–CH=N–CH$_2$–C$_6$H$_5$]Fe(η^5 - C$_5$H$_5$)}-(μ-Cl)]$_2$ [1] (157 mg, 1.67×10^{-4} mol) was suspended in 30 cm^3 of methanol. Then a solution containing 56 mg (3.37×10^{-4} mol) of KI in methanol (25 cm^3) was added. The resulting mixture was stirred at room temperature (r.t.) ca. 20°C, for 1 h. The solid formed was collected by filtration and air-dried (yield: 79.7%). Characterization data: Anal. Calc. for: C$_{36}$H$_{32}$Fe$_2$I$_2$N$_2$Pd$_2$ (Found): C, 40.37 (40.4); H, 3.01 (3.1) and N, 2.62 (2.55)%. IR: ν(>C=N–) = 1580 cm^{-1}.

3.1.2. Preparation of [Pd{[(η^5-C$_5$H$_3$)–CH=N–CH$_2$-C$_6$H$_5$]Fe(η^5-C$_5$H$_5$)}(μ–AcO)]$_2$

The ferrocenylketimine: [(η^5-C$_5$H$_5$)Fe{(η^5-C$_5$H$_3$)–CH=N–CH$_2$–C$_6$H$_5$}] (1.01 g, 3.3×10^{-3} mol), Pd(AcO)$_2$ (0.747 g, 3.3×10^{-3} mol) and NaAcO·3H$_2$O (0.450 g, 3.3×10^{-3} mol) were suspended in 40 cm^3 of methanol. The reaction mixture was protected from light with aluminium foil and stirred at r.t. (ca. 20°C) for 24 h. After this period the red solid formed was

collected by filtration and washed with three portions of 5 cm^3 of methanol. The solid was air-dried and then dried in vacuum (yield: 67%). Characterization data: Anal. Calc. for: $C_{40}H_{38}Fe_2N_2O_4Pd_2$ (Found): C, 51.37 (51.45); 4.10 (4.15) and N, 3.00 (2.9)%. IR: $v(>C=N-)$ = 1590 cm^{-1} (br).

3.1.3. Preparation of [Pd{[(η⁵-C₅H₃)–CH=N–CH₂–C₆H₅]Fe(η⁵-C₅H₅)(Br)(PPh₃)]

A 105 mg (1.50×10^{-4} mol) amount of [Pd{[(η⁵-C₅H₃)–CH=N–CH₂–C₆H₅]Fe(η⁵-C₅H₅)(Cl)(PPh₃)] was dissolved in 20 cm^3 of acetone, then AgNO₃ (25.5 mg, 1.50×10^{-4} mol) was added. The reaction mixture was protected from the light with aluminium foil and stirred at rt. ca. 20°C for 30 min. After this, the solution was filtered out to remove the AgCl formed and the filtrate was treated with 150×10^{-4} mol of KBr. The reaction mixture was stirred at r.t. for 2 h. The resulting red solution was filtered out and the filtrate was then concentrated to dryness on a rotary evaporator. The residue was dissolved in the minimum amount of CH_2Cl_2 and passed through an SiO_2 column using CH_2Cl_2 as eluant. The red band released was collected and concentrated in a rotary evaporator to ca. 2 cm^3. The red cubes formed upon cooling were collected by filtration and air-dried (yield: 72%). Characterization data: Anal. Calc. for: $C_{36}H_{31}BrFeNPPd$ (Found): C, 57.59 (57.6); H, 4.16 (4.2) and N, 1.87 (1.9)%. IR: $v(>C=N-)$ = 1585 cm^{-1}.

3.1.4. Preparation of [Pd{[(η⁵-C₅H₃)–CH=N–CH₂–C₆H₅]Fe(η⁵-C₅H₅)}I(PPh₃)]

Triphenylphosphine (45 mg, 1.72×10^{-4} mol) was added to a suspension formed by 93 mg (8.9×10^{-5} mol) of [Pd{[(η⁵-C₅H₃)–CH=N–CH₂–C₆H₅]Fe(η⁵-C₅H₅)}(μ-I)]₂ and 10 cm^3 of acetone. The resulting mixture was refluxed for 30 min. After this period the undissolved materials were removed by filtration and discarded, and the filtrate was concentrated to dryness on a rotary evaporator. The residue was then dissolved in the minimum amount of CH_2Cl_2 and passed through a SiO_2 column chromatography. Elution with CH_2Cl_2 produced the release of a red band which was collected and concentrated in a rotary evaporator to ca. 3 cm^3. The solution was then treated with *n*-hexane (ca. 5 cm^3). Slow evaporation of the solvent produced small red cubes which were collected and air-dried (yield: 58%). Anal. Calc. for $C_{36}H_{31}NFeIPdP\cdot1/4CH_2Cl_2$ (found): C, 53.11 (52.9); H, 3.90 (3.85) and N, 1.70 (1.8)%. IR: $v(>C=N-)$ = 1587 cm^{-1}.

3.1.5. Preparation of [Pd{[(η⁵-C₅H₃)–CH=N–CH₂–C₆H₅]Fe(η⁵-C₅H₅)}(X)(PPh₃)] with X⁻ = CN⁻ or SCN⁻

These compounds were prepared according to the procedure described above for [Pd{[(η⁵-C₅H₃)–CH=N–CH₂–C₆H₅]Fe(η⁵-C₅H₅)}(Br)(PPh₃)], but using the stoichiometric amount of KCN or KSCN (yields: 68 and 62%, respectively). Characterization data: for [Pd{[(η⁵-C₅H₃)–CH=N–CH₂–C₆H₅]Fe(η⁵ - C₅H₅)}(CN)(PPh₃)]: Anal. Calc. for $C_{37}H_{31}N_2FePPd$ (Found): C, 63.77 (63.9); H, 4.48 (4.5) and N, 4.01 (3.9)%. IR: $v(>C=N-)$ = 1597 cm^{-1} and $v(SCN)$ = 2145 cm^{-1} and. For [Pd{[(η⁵ - C₅H₃)–CH=N–CH₂–C₆H₅]Fe(η⁵ - C₅H₅)}-(SCN)(PPh₃)]: Anal. Calc. for $C_{37}H_{31}N_2FePdPS\cdot1/2CH_2Cl_2$ (Found): C, 58.39 (58.55); H, 4.18 (4.25); N, 3.63 (3.7) and S, 4.16 (4.2)%. IR: $v(>C=N-)$ = 1590 cm^{-1} and $v(CN)$ = 2091 cm^{-1}.

3.1.6. Preparation of [Pd{[(η⁵-C₅H₃)–CH=N–CH₂–C₆H₅]Fe(η⁵-C₅H₅)}(AcO)(PPh₃)]

Compound [Pd{[(η⁵-C₅H₃)–CH=N–CH₂–C₆H₅]Fe-(η⁵-C₅H₅)}(μ-AcO)]₂ (130 mg, 1.39×10^{-4} mol) was suspended in 40 cm^3 of acetone. Then, 73 mg (2.79×10^{-4} mol) of PPh₃ were added. The reaction mixture was refluxed for 30 min. After cooling to room temperature (ca. 20°C), it was filtered out and the filtrate was concentrated to dryness on a rotary evaporator giving a deep red residue, which was later dissolved in the minimum amount of CH_2Cl_2 and passed through an SiO_2 column chromatography. Elution with CH_2Cl_2 released a red band which was collected and concentrated to dryness on a rotary evaporator. The solid formed was collected and air-dried (yield: 58%). Characterization data: Anal. Calc. for: $C_{38}H_{34}NFeO_2PPd$ (Found): C, 62.53 (62.6), H, 4.70 (4.75) and N, 1.92 (2.0)%. IR: $v(>C=N-)$ = 1594 cm^{-1}, $v(CO_2)$ = 1619 and 1341 cm^{-1}

3.2. Crystallography

A prismatic crystal (sizes in Table 5) of [Pd{[(η⁵-C₅H₃)–CH=N–CH₂–C₆H₅]Fe(η⁵ - C₅H₅)}(X)(PPh₃)] with X⁻ = Br⁻ or I⁻ was selected and mounted on a Enraf-Nonius CAD4 four-circle diffractometer. Unit-cell parameters were determined from automatic centring of 25 reflections in the range $12 = \Theta = 21°$ and refined by least-squares method. Intensities were collected with graphite monochromatized Mo–K$_\alpha$ radiation using $\omega/2\Theta$ scan technique. For the bromo derivative, 8985 reflections were measured in the range $2.32 \leq \Theta \leq 29.96°$, of which 8924 were non-equivalent by symmetry [R_{int}(on I) = 0.016]; while for: [Pd{[(η⁵-C₅H₃)–CH=N–CH₂–C₆H₅]Fe(η⁵ - C₅H₅)}(I)(PPh₃)], 9012 reflections were collected in the range $2.38 \leq \Theta \leq 29.96°$, of which 8950 were non-equivalent by symmetry [R_{int}(on I) = 0.017]. The number of reflections assumed as observed, applying the condition $I > 2\sigma(I)$, was 6062 for X⁻ = Br⁻ and 6065 for X⁻ = I⁻. In the two cases, three reflections were measured every 2 h as orientation and intensity control, and no significant intensity decay was observed. Lorentz polarization and absorption corrections were made.

The structures were solved by direct methods using the SHELXS computer program [17] and refined by full-matrix least-squares method with the SHELX-97 computer program [18] using 8924 reflections (very negative intensities were not assumed). The function minimized was $\Sigma w||F_o|^2 - |F_c|^2|^2$, where $w = [\Theta^2(I) + (0.0475P)^2 + 0.0403P]^{-1}$ (for $X^- = Br^-$) and $[\sigma^2(I) + (0.0631P)^2]^{-1}$ (for $X^- = I^-$) and $P = (|F_o|^2 + 2|F_c|^2)/3$. f, f' and f'' were taken from the literature [19]. For $[Pd\{[(\eta^5 - C_5H_3)-CH=N-CH_2-C_6H_5]Fe(\eta^5 - C_5H_5)\}(Br)(PPh_3)]$, all hydrogen atoms were located from a difference synthesis and refined with an overall isotropic temperature factor, while for $[Pd\{[(\eta^5-C_5H_3)-CH=N-CH_2-C_6H_5]Fe(\eta^5-C_5H_5)\}(Br)(PPh_3)]$ 27 hydro-

gen atoms were located from a difference syntheses and refined with an overall isotropic temperature factor. The remaining four hydrogen atoms were computed and refined with an overall isotropic temperature factor equals to 1.2 times the equivalent isotropic temperature factor of the atoms attached using a riding model. The final R (on F) factors were 0.043 (for $X^- = Br^-$) and 0.042 (for $X^- = I^-$) and wR (on $|F|^2$) values were 0.087 and 0.098 for compounds having $X^- = Br^-$ and I^-, respectively. The goodness of fit was 1.025 (for $X^- = Br^-$) and 1.034 (for $X^- = I^-$) for all the observed reflections. Further details concerning the resolution and the refinement of the crystal structure are shown in Table 5.

3.3. Computational details

The calculations were performed using the SPARTAN 5.0 suite of programs [15] on a Silicon Graphics workstation (INDIGO-2 power ZX). The PM3(tm) method was used with the default parameters provided by the program. The crystallographic coordinates of $[Pd\{[(\eta^5-C_5H_3)-CH=N-CH_2-C_6H_5]Fe(\eta^5-C_5H_5)\}(X)(PPh_3)]$ ($X = Br^-$ or I^-) were used as input for the program, and the Br^- group was then replaced by the corresponding monoanionic ligand $\{Cl^-, I^-, CN^-$ or $SCN^-\}$. Then, the geometry of all the compounds was optimized before the calculations. No significant variations were detected in the bond lengths and angles of the optimized geometry and the structural data available for the complexes $[Pd\{[(\eta^5-C_5H_3)-CH=N-CH_2-C_6H_5]Fe(\eta^5-C_5H_5)\}(X)(PPh_3)]$ (with $X^- = Cl^-$ [19], Br^- or I^-). Geometrical restrictions were not imposed in any case.

Table 5
Crystal data and details of the refinement of the crystal structure of compounds $[Pd\{[(\eta^5-C_5H_3)-CH=N-CH_2-C_6H_5]Fe(\eta^5-C_5H_5)\}(X)(PPh_3)]$ with $X^- = Br^-$ or I^-

	$X^- = Br^-$	$X^- = I^-$
Empirical fomula	$C_{36}H_{31}BrFeNPPd$	$C_{36}H_{31}IFeNPPd$
Formula weight	750.75	797.74
Crystal size (mm)	$0.1 \times 0.1 \times 0.2$	$0.1 \times 0.1 \times 0.2$
Temperature (K)	293(2)	293(2)
Wavelength (Å)	0.71069	0.71069
Crystal system	Triclinic	Triclinic
Space group	$P\bar{1}$	$P\bar{1}$
a (Å)	10.908(9)	11.037(2)
b (Å)	11.066(2)	11.061(5)
c (Å)	13.258(4)	13.412(11)
α (°)	85.66(2)	89.15(5)
β (°)	88.93(4)	81.15(4)
γ (°)	73.67(4)	73.07(3)
V (Å^{-3})	1531.4(14)	1562.8(15)
Z	2	2
D_{calc} (mg m^{-3})	1.628	1695
Absorption coefficient (mm^{-1})	2.444	2.104
$F(000)$	752	788
θ Range for data collection (°)	2.32 to 29.96	2.38 to 29.96
Index ranges	$-15 \leq h \leq 15$, $-15 \leq k \leq 15$, $0 \leq l \leq 18$	$-15 \leq h \leq 15$, $-15 \leq k \leq 15$, $0 \leq l \leq 18$
No. of reflections collected	8985	9012
No. of unique reflections	8924 [$R_{int} = 0.0164$]	8950 [$R_{int} = 0.0171$]
Completeness to $2\Theta = 29.96°$	100.0%	98.3%
Refinement method	Full-matrix least-squares	Full-matrix least-squares
No. of data	8924	8950
No. of parameters	494	478
Goodness-of-fit on F^2	1.025	1.034
R indices [$I = 2\sigma(I)$]	$R_1 = 0.0431$, $wR = 0.0877$	$R_1 = 0.0428$, $wR = 0.0981$
R indices (all data)	$R_1 = 0.0949$, $wR_2 = 0.1010$	$R_1 = 0.0739$, $wR_2 = 0.1094$
Largest difference peak and hole (e Å^{-3})	0.883 and -0.686	0.556 and -0.425

4. Supplementary material

Crystallographic data for the structural analysis have been deposited with the Cambridge Crystallographic Data Centre, CCDC nos. 149875 and 149876 for compounds with $X^- = Br^-$ or I^-, respectively. Copies of this information may be obtained from The Director, CCDC, 12 Union Road, Cambridge, CB2 1EZ, UK (fax: $+44$-1233-336033; e-mail: deposit@ccdc.cam.ac.uk or www: http://www.ccdc.cam.ac.uk).

References

[1] C. López, J. Sales, X. Solans, R. Zquiak, J. Chem. Soc. Dalton Trans. (1992) 2321.

[2] R. Bosque, C. López, J. Sales, X. Solans, M. Font-Bardía, J. Chem. Soc. Dalton Trans. (1994) 735.

[3] R. Bosque, M. Font-Bardía, C. López, J. Sales, X. Solans, J. Silver, J. Chem. Soc. Dalton Trans. (1994) 746.

[4] C. López, R. Bosque, X. Solans, M. Font-Bardía, D. Tramuns, G. Fern, J. Silver, J. Chem. Soc. Dalton Trans. (1994) 3039.

[5] R. Bosque, C. López, J. Sales, Inorg. Chim. Acta 244 (1996) 141.

[6] C. López, R. Bosque, X. Solans, M. Font-Bardía, New J. Chem. 22 (1998) 977.

[7] W.A. Henderson, C.A. Screuli, J. Am. Chem. Soc. 82 (1960) 5791.

[8] C. Hansch, A. Leo, D. Hoekman, Exploring QSAR: Hydrophobic, Electronic and Steric Constants, American Chemical Society, Washington, DC, 1995.

[9] K. Nakamoto, Infrared Spectra of Inorganic and Coordination Compounds, 3rd edn., Wiley, New York, 1978.

[10] (a) G.B. Deacon, R.J. Phillips, Coord. Chem. Rev. 33 (1989) 227. (b) G.B. Deacon, F. Huber, R.J. Phillips, Inorg. Chim. Acta 104 (1985) 41.

[11] (a) J. Albert, J. Granell, J. Sales, M. Font-Bardía, X. Solans, Organometallics 14 (1995) 1393. (b) J. Albert, J. Granell, R. Moragas, M. Font-Bardía, X. Solans, J. Organomet. Chem. 522 (1996) 59. (c) J. Albert, M. Gómez, J. Granell, J. Sales, Organometallics 9 (1990) 1405.

[12] C. López, R. Bosque, X. Solans, M. Font-Bardía, New. J. Chem. 20 (1996) 1285.

[13] (a) A. Bondi, J. Phys. Chem. 68 (1964) 441. (b) A.I. Kitaigorodskii, Molecular Crystals and Molecules, Academic Press, London, 1973.

[14] C. López, R. Bosque, X. Solans, M. Font-Bardía, D. Tramuns, G. Fern, J. Silver, J. Chem. Soc. Dalton Trans. (1994) 747.

[15] SPARTAN 5.0. Wavefunction Inc. Irvine, CA, 1995.

[16] I. Mayer, Chem. Phys. Lett. 97 (1983) 270.

[17] G.M. Sheldrick, SHELXS, A computer program for determination of crystal structure, University of Göttingen, Germany, 1997.

[18] G.M. Sheldrick, SHELX-97, A computer program for determination of crystal structure, University of Göttingen, Germany, 1997.

[19] International Tables of X-ray Crystallography, vol. IV, Kynoch Press (Ed.), Birmingham, 1974, pp. 99, 100 and 149